36th UK Group Conference on Human Response to Vibration

12 - 14 September, 2001

Centre for Human Sciences
QinetiQ Ltd, Farnborough
England

MODELING OF BIOMECHANICS OF TWO-POINT DISCRIMINATION TESTS OF FINGERTIP

J.Z. Wu[1], R.G. Dong[1], S. Rakheja[2], A.W. Schopper[1], and W.P. Smutz[1]
[1]National Institute for Occupational Safety & Health (NIOSH)
Morgantown, West Virginia 26505, USA
[2]CANCAVE Research Center, Concordia University
Montreal, Quebec H3G 1M8, CANADA

Abstract

A two-dimensional model is proposed that incorporates the essential anatomical structures of a finger: skin, subcutaneous tissue, bone, and nail. The skin tissue is assumed to be hyperelastic and viscoelastic. The subcutaneous tissue is considered to be a nonlinear, biphasic material composed of a hyperelastic solid and an invicid fluid phase. The nail and bone are considered to be linearly elastic. The proposed model is applied to simulate the mechanical responses of a fingertip in one-point (1PT) and two-point (2PT) tactile discrimination tests. In case of wo-point tests, the effects of static and dynamic indentations on the stress/strain distributions within the soft tissues at fingertip have been studied numerically. Assuming that mechanoreceptors in the dermis sense the stimuli associated with normal strains (the vertical and horizontal strains) and strain energy density, our numerical results suggest that the threshold of 2PT discrimination may lie between 2.0 mm and 3.0 mm, which is consistent with the published experimental data.

1. Introduction

The tactile senses, in general, include the sensation of touch, pressure, vibration, and temperature. Humans primarily use their fingertips in exploration of external world through the sense of touch. The tactile receptors beneath the skin respond to deformation of the skin by transmitting electrical impulses to the brain through peripheral nerve systems, when the fingertips come in contact with an object (Guyton, 1982). The primary features of transmitted signals, such as frequencies of nerve impulses, are associated with mechanical environment of the tactile receptors, e.g., stress and strain (Srinivasan and LaMotte, 1987). The presence of multiple mechanoreceptors that respond to mechanical stimuli in different manners has been reported by Verrillo and Gescheider (1977). The study of biomechanics of the fingertips is vital to enhance an understanding of mechanism of tactile sensation and sensory thresholds.

The soft subcutaneous and skin tissues are known to exhibit nonlinear and time-dependent material properties (Zheng and Mak, 1996; Rubin et al., 1998; Wan, 1994), and, consequently, the responses of fingertips to mechanical loading are expected to be nonlinear and time-dependent. Since the

Presented at the 36th United Kingdom Group Conference on Human Response to Vibration, held at Centre for Human Sciences, QinetiQ, Farnborough, UK, 12 - 14 September 2001

tactile sensation is known to depend on the nature of the mechanical stimuli (frequency and magnitude), contact force and contact area (Harada and Griffin, 1991), the effects of nonlinearity and time-dependency of the soft tissues are expected to have substantial influences on the vibrotactile sensation and tactile performances, which are related to activity of nerve endings at the fingertips, and sensitivity of soft subcutaneous tissue to skin indentation. The reported fingertip models (Phillip and Johnson, 1981; Srinivasan and Dandekar, 1996; Serina et al., 1998) do not incorporate the nonlinear and time-dependent effects associated with the anatomical substructures and tissue material properties. The purpose of the present research is to develop a model based on finite element techniques to simulate the mechanics of tactile sensation of a fingertip. A two-dimensional model is proposed that incorporates the essential anatomical structures of a finger: skin, subcutaneous tissue, arterial bone, and nail. The skin tissue is assumed to be hyperelastic and viscoelastic. The subcutaneous tissue is considered to be a nonlinear, biphasic material composed of a hyperelastic solid and an invicid fluid. The hydraulic permeability of the subcutaneous tissue is considered to be deformation dependent. The mechanical responses of a fingertip in one-point (1PT) and two-point (2PT) tactile discrimination tests are simulated using the proposed model.

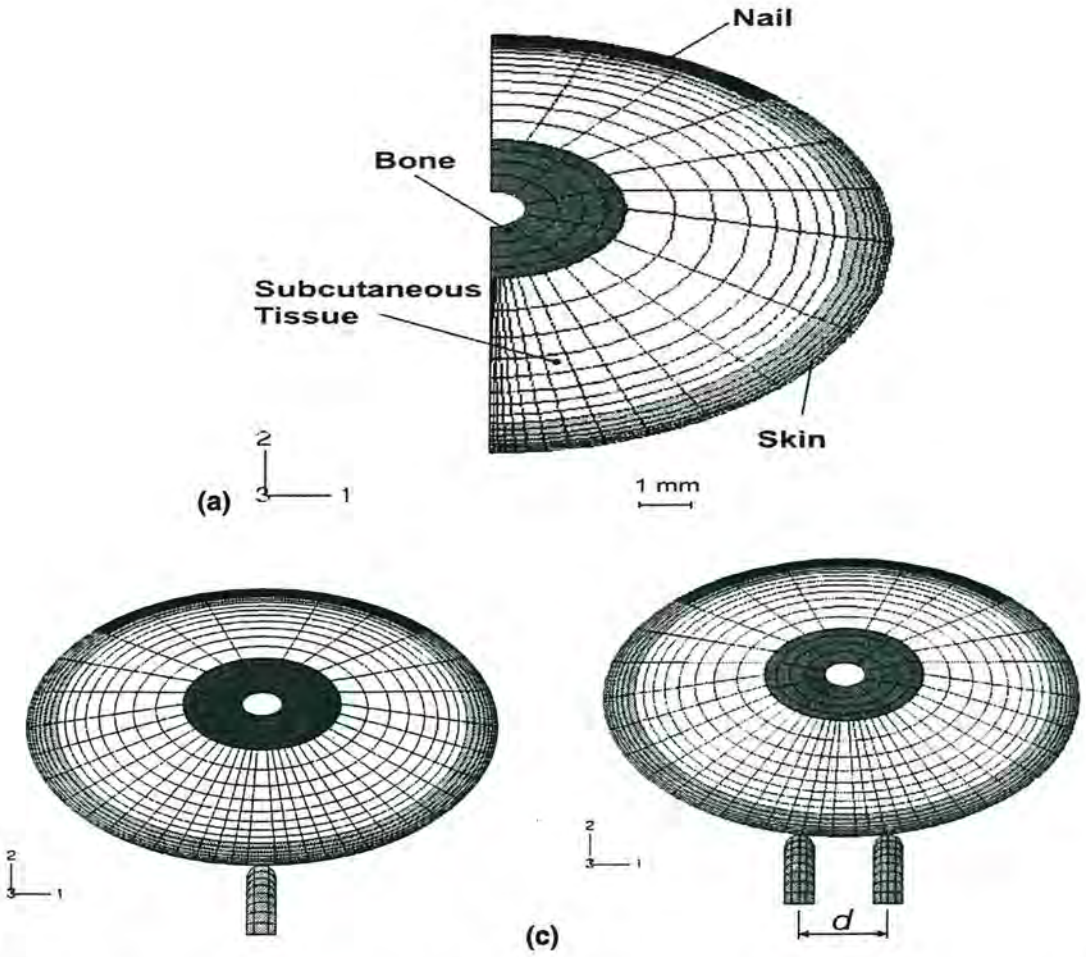

Figure 1: (a): Finite element modelling of fingertip. (b): One-point (1PT) indentation test. (c): Two-point (2PT) indentation test.

The biomechanics of tactile sensation of a fingertip is analysed using a multi-layered two-dimensional finite element model, as shown in Fig.1(a). The fingertip is assumed to be composed of a skin layer (representing epidermis and dermis), subcutaneous tissue, bone, and nail. The fingertip dimensions are assumed to be representative of index finger of a male subject (Clemente, 1981). The skin is assumed to have a thickness of 0.8 mm. The cross section of the fingertip and the bone are assumed to be elliptical and the tissue thickness is considered to be asymmetric about the bone [Fig.1(a)]; the tissue thickness between the bone and the pulp skin surface is assumed to be larger than that between the bone and the nail. The biquadral, plain-strain elements were used in the finite element models. The commercial finite element software package Abaqus (version 6.1) was applied for the analysis.

The skin tissue, including epidermis and dermis, is assumed to be hyperelastic and linearly viscoelastic. The subcutaneous tissue is assumed to be a biphasic material composed of a fluid phase and a hyperelastic solid phase. The nail and the bone are considered as linearly elastic. The constitutive equations of the skin and subcutaneous tissue and the material parameters used in the present simulations are given in the Appendix.

Numerical tests are performed to study the mechanics of tactile sensation of the fingertip in one-point (1PT) and two-point (2PT) discrimination tests. The fingertip was fixed on the center of the nail surface, while either one or two indentors (each with a circular contact surface and thickness of 1 mm) were used to deform the skin surface of the fingertip by 1 mm within a ramping period of 1 s [Figs.1(b) and 1(c)]. A total of five numerical tests were performed, where the first test was carried out using one single indentor [Fig.1 (b)]. The remaining four tests were performed using two indentors with different spacing between the indentors [Fig.1 (c)]: d = 1.5, 2.0, 3.0, and 4.0 mm, respectively. The analyses were performed to compute the displacement, stress, and strain fields within the soft tissue at the state of maximum depression. Merkel cell receptors associated with SAI fibers were reported to be embedded at a depth of approximately 0.5-1.0 mm from the skin surface (Srinivasan and Dandekar, 1996), therefore, the mechanical states (stress/strain) of the tissue at a depth of 0.75 mm during the indentation tests are analyzed in the present study.

3. Results

Fig. 2 illustrates distribution of vertical displacements of the tissue at a depth of 0.75 mm from the undeformed skin surface under one-point (1PT) and two-point (2PT) indentations. The figure also illustrates the deflection responses as a function of the indentor spacing d in case of 2PT indentation. The peak displacements occur at contact points for both 1PT and 2PT indentations. In case of 2PT indentation, the differences between displacement at the center and those at the contact points increase with increased spacing between the indentors (d).

The distributions of strains in the horizontal and vertical directions at a depth of 0.75 mm from the undeformed skin surface for 1PT and 2PT indentations are illustrated in Figs. 3(a) and 3(b), respectively. The differences between the strain values at the center and those at the contact points

decrease in general with decrease in spacing between the indentors (d). It is interesting to note that, the positive peak values of the horizontal strains [Fig. 3(a)] and the negative peak values of the vertical strains [Fig. 3(b)] vary only slightly in the vicinity of the contact points, when spacing between the indentors decreased from 4.0 mm to 1.5 mm. The corresponding strain values at the center of the fingertip changed slightly when spacing between the indentors is reduced from 4.0 mm to 2.0 mm. A further reduction in the indentor spacing (d= 1.5 mm), however, yields significant variation in the strain values, as indicated in Figs.3(a) and 3(b).

The distribution of the shear strain and strain energy density at a depth of 0.75 mm from the undeformed skin surface, derived from 1PT and 2PT indentation models, are illustrated in Figs. 4(a) and 4(b), respectively. The shear strain profiles reverse direction near contact points, and peak-to-peak variations in the strain around the contact point decrease dramatically when indentor spacing decreases from 4.0 mm to 1.5 mm, as shown in Fig. 4(a). The magnitudes of the strain energy density approach their peak values under contact points, and these peak values decrease when the indentor spacing decreases from 4.0 mm to 1.5 mm.

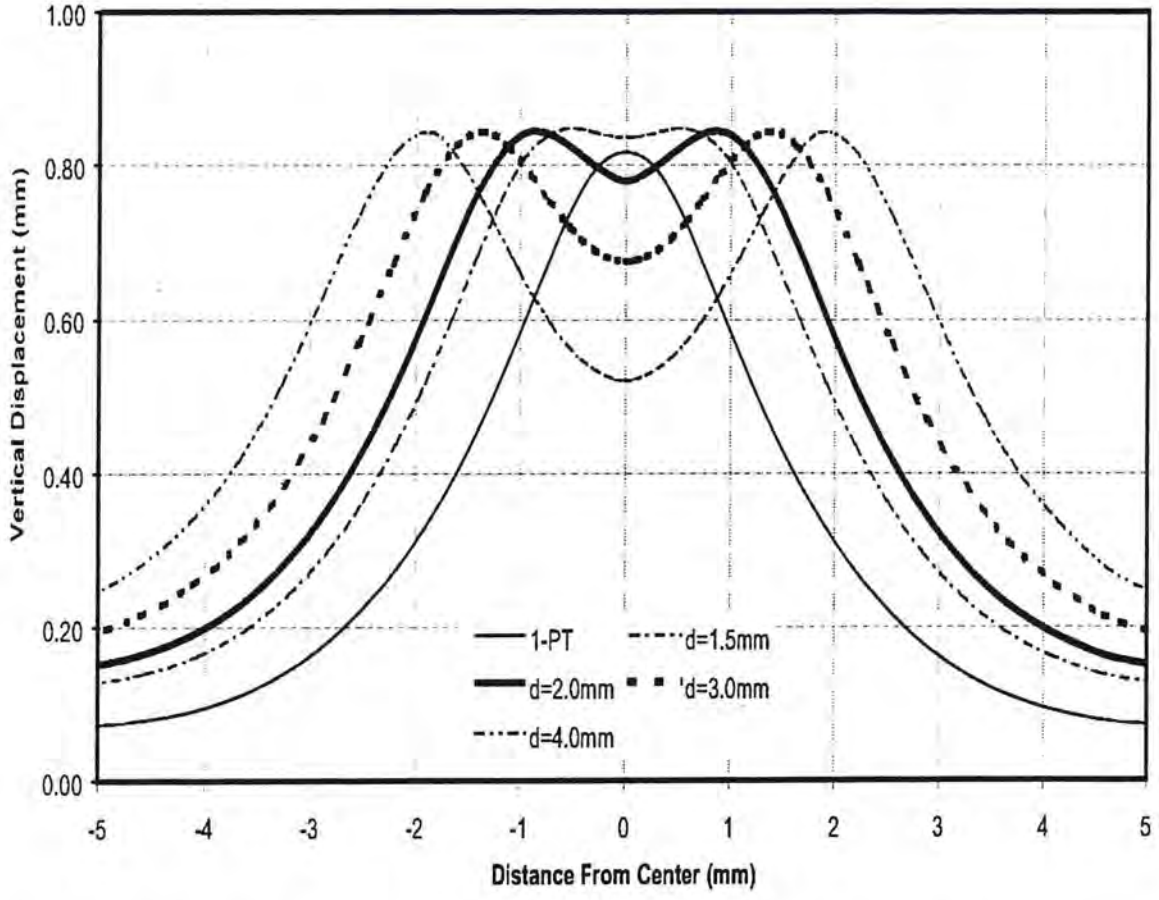

Figure 2: Predicted distributions of vertical displacement in the soft tissue of fingertip (at a depth of 0.75 mm from the undeformed skin surface) for 1PT and 2PT tests (t=*1 s*).

(a)

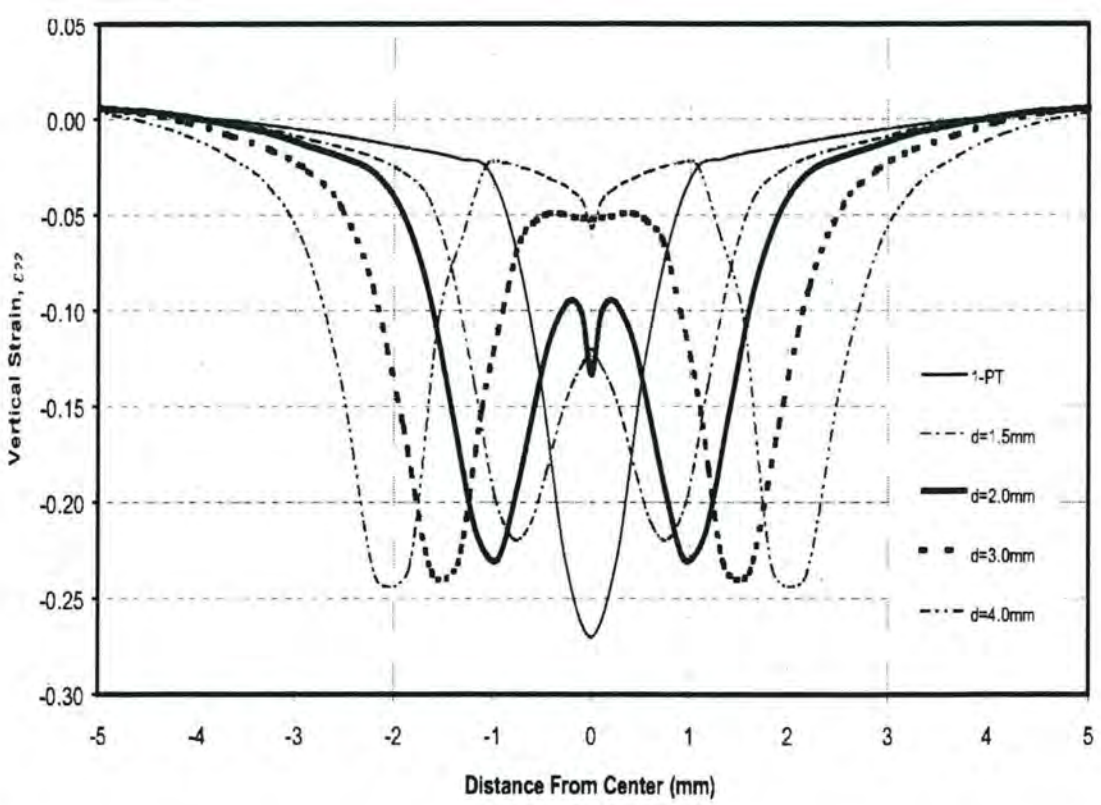

(b)

Figure 3: Predicted distributions of strains in the soft tissue of fingertip (at a depth of 0.75 mm from the undeformed skin surface) for 1PT and 2PT tests (*t=1 s*). (a): horizontal strain. (b): vertical strain.

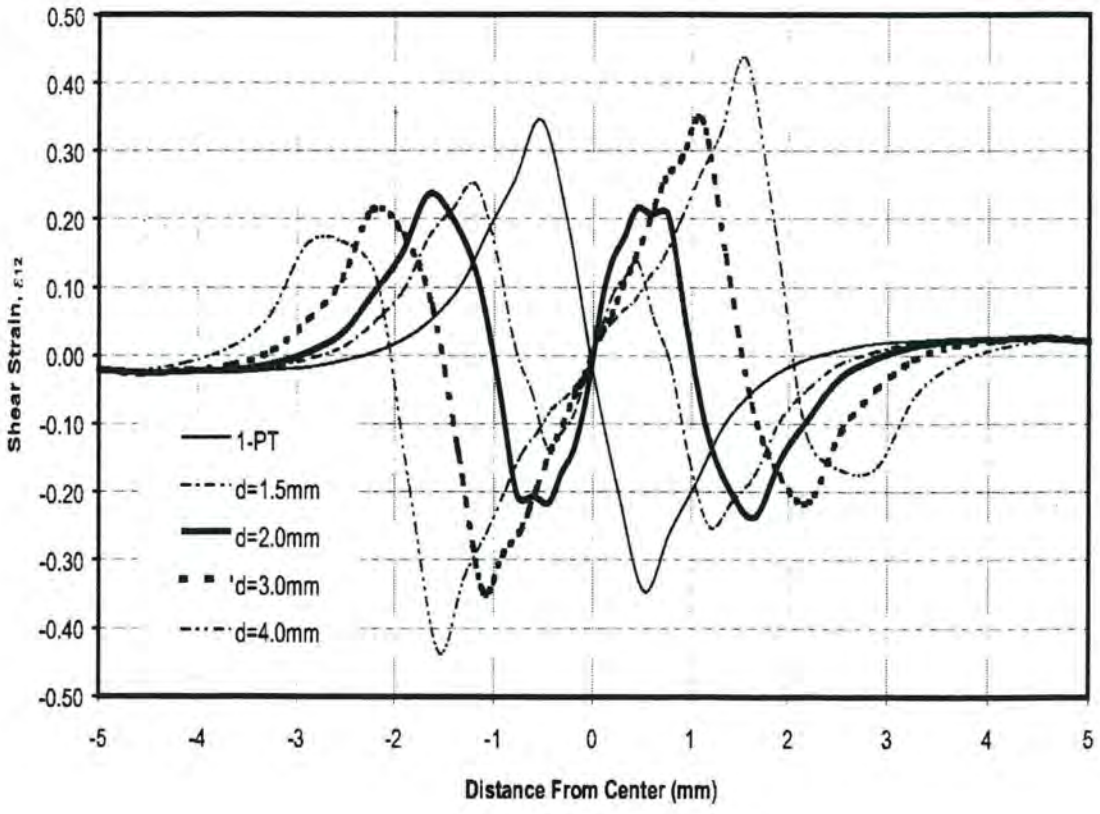

(a)

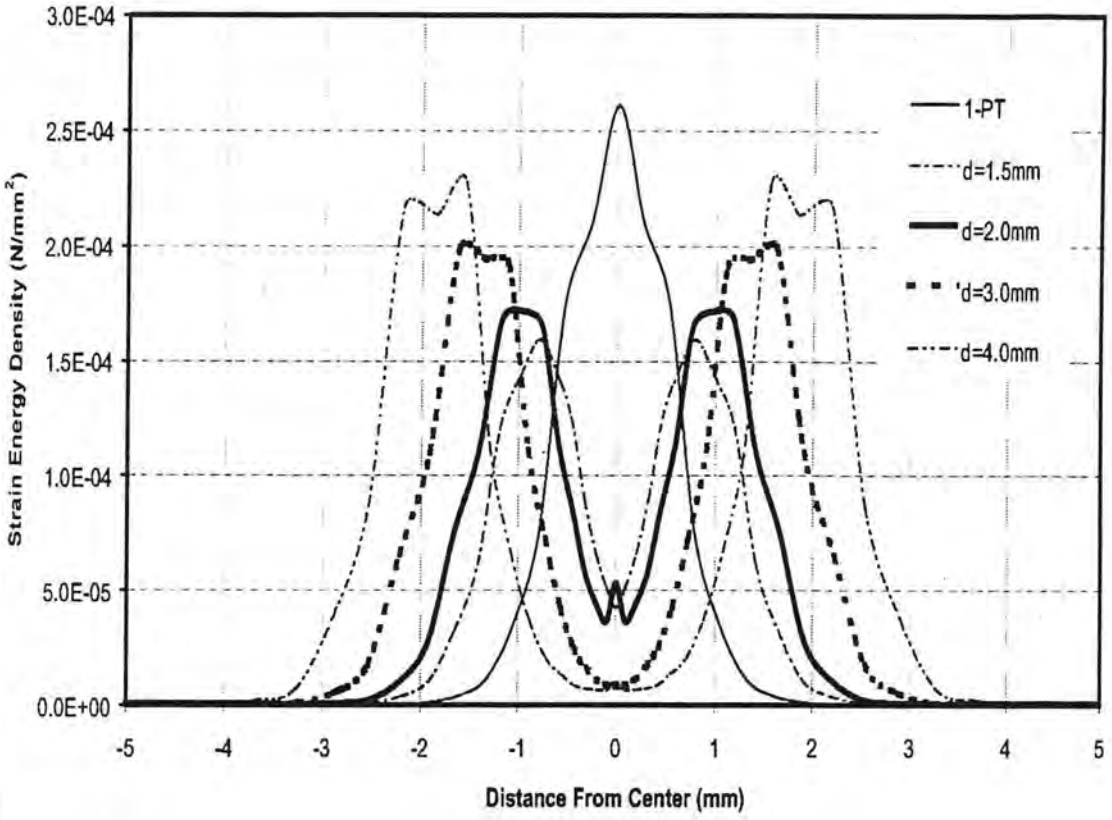

(b)

Figure 4: Predicted distributions of the shear strains and strain energy density in the soft tissue of fingertip (at a depth of 0.75 mm from the undeformed skin surface) for 1PT and 2PT tests (*t=1 s*). (a): The shear strain. (b): The strain energy density.

5. Discussion and Conclusion

The tactile sensation of the human fingertips has been widely used for assessment of health effects associated with prolonged exposure to hand-transmitted vibration (ISO-13091-1, 2001) and carpal tunnel syndrome (Morissey et al., 1996). The tactile performance is associated with activities of the nerve endings of the fingertips and sensitivity of the soft tissue within the fingertip to the nature of static and dynamic skin indentation. In the present study, a FE model of a fingertip is developed on the basis of anatomical structures to investigate biomechanics of the tactile sensation. The advantages of the proposed fingertip model over the previous "waterbed" (Serina et al., 1998) and continuous fingertip models (Phillip and Johnson, 1981; Srinivasan and Dandekar, 1996) include its abilities to predict the surface deflection of the fingertip, stress and strain distributions within the soft tissue, and, most importantly, the dynamic responses of the fingertip to mechanical stimuli.

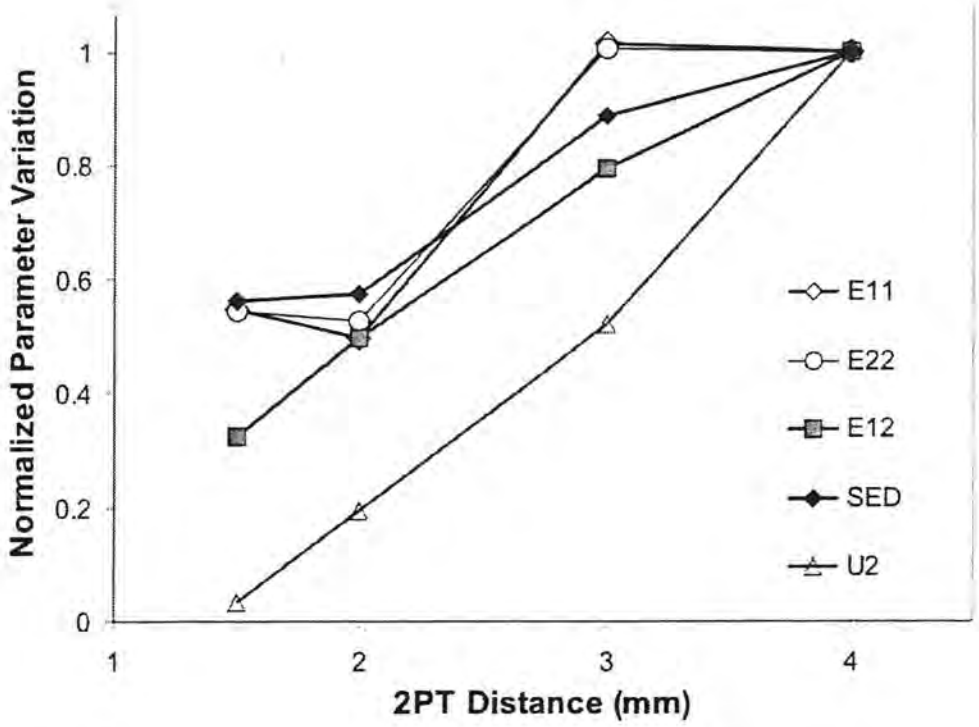

Figure 5: Normalized variations of horizontal (*E11*), vertical (*E22*) and shear strains (*E12*), vertical displacement (*U2*), and strain energy density (*SED*) as a function of 2PT spacing. The normalized variations were evaluated by $[\, f_{\text{(contact point of indentor)}} - f_{\text{(geometry center)}}]/\, f_{\text{(contact point of indentor)}}$ with f= *E11, E22, E12, U2,* and *SED*, as shown in Figs. 2-4.

The model results for the 2PT discrimination tests reveal that differences in normal strains (horizontal and vertical strains) and strain energy density developed in the skin at the contact points and at the geometric center of the fingertip vary only slightly with a decrease in the indentor spacing from 4.0 to 3.0 mm (Fig. 5). These differences, however, decrease considerably with a further decrease in the indentor spacing from 3.0 to 2.0 mm (Fig. 5). The corresponding differences in the vertical displacement and shear strain, however, decreased almost linearly with decrease in the indentor spacing from 4.0 to 1.5 mm. Assuming that mechanoreceptors in the dermis sense the stimuli associated with normal strains (horizontal and vertical strains) and train energy density rather than those associated with shear train, the possibly lowest bound of threshold of 2PT discrimination test for the fingertip may lie between 2.0 and .0 mm based on the present analysis. This observation is consistent with the experimental observations reported by Perez et al. (2000) who reported an average 2PT discrimination distance of 2.1 mm in vibrotactile tests of the index finger.

6. APPENDIX

Constitutive Equation for the Skin

The skin (epidermis and dermis) is assumed to experience large deformation and possess nonlinearly elastic and linearly viscoelastic properties. The total tissue stress ($\tilde{\sigma}$) is assumed to be composed of elastic ($\tilde{\sigma}^0$) and viscous ($\tilde{\sigma}^v$) stress components, such that:

$$\tilde{\sigma}(t) = \tilde{\sigma}^0(t) + \tilde{\sigma}^v(t) = \tilde{\sigma}^0(t) + \int_0^t \frac{\dot{G}(\tau)}{G_0} \tilde{\sigma}^0(t-\tau)d\tau = \tilde{\sigma}^0(t) + \int_0^t \dot{g}(\tau)\tilde{\sigma}^0(t-\tau)d\tau \qquad (1)$$

where *t* is time. The stress relaxation function is defined using the Prony series (Tschoegl, 1989)

$$g(t) = \frac{G(t)}{G_0} = \left[1 - \sum_{i=1}^{N_G} g_i \left(1 - e^{\frac{t}{\tau_i}}\right)\right] \qquad (2)$$

where G_0 and $G(t)$ are the instantaneous and time-dependent moduli, respectively; g_i and τ_i ($i=1,2,..$ N_G) are stress relaxation parameters; N_G is the number of terms used in the stress relaxation function.

The elastic deformation behaviour of the soft tissue, based on finite deformation theory, is assumed to be nonlinearly elastic (hyperelastic). A function of strain energy density per unit volume, *U*, defined for the elastometric foams (Storakers, 1986) is applied to describe the elastic behaviour of the tissue in the following manner:

$$U = \sum_{i=1}^{N} \frac{2\mu_i}{\alpha_i^2}\left[\lambda_1^{\alpha_i} + \lambda_2^{\alpha_i} + \lambda_3^{\alpha_i} - 3 + \frac{1}{\beta}\left(J^{-\alpha_i\beta} - 1\right)\right] \qquad (3)$$

where $J = \lambda_1\lambda_2\lambda_3$ is the volume ratio, λ_i ($i=1,2,3$) are the principal stretch ratios, α_i and μ_i ($i=1,..$ N) are the material parameters, $\beta=\nu/(1-2\nu)$ where ν is the Poisson's ratio, and N is the number of terms used in the strain energy function.

The elastic stress $\tilde{\sigma}_0$ is related to the elastic strain energy function (3) by

$$\tilde{\sigma}_0 = 2\tilde{F}\frac{\partial U}{\partial \tilde{C}}\tilde{F}^T \qquad (4)$$

where $\tilde{F}$ and $\tilde{C}$ are the deformation gradient and the right Cauchy-Green deformation tensors, respectively.

Constitutive Equation for the Subcutaneous Tissue

The subcutaneous tissue is modeled as a sponge-like porous material fully saturated with fluid. The biphasic models for articular cartilage (Mow et al., 1980; Holmes and Mow, 1990) are adopted in the

subcutaneous tissue undergoes large deformation, the poroelastic constitutive relation is formulated based on the finite deformation theory with a deformation-dependent hydraulic permeability. The tissue stress, $\tilde{\sigma}^t$, is composed of the stresses in the solid and fluid phase, $\tilde{\sigma}^s$ and $\tilde{\sigma}^f$, respectively:

$$\tilde{\sigma}^t = \tilde{\sigma}^f + \tilde{\sigma}^s; \quad \tilde{\sigma}^f = -\Phi^f p\tilde{I}, \quad \tilde{\sigma}^s = \tilde{\sigma}_0{}^s - \Phi^s p\tilde{I} \tag{5}$$

where Φ^s and Φ^f, with $\Phi^f + \Phi^s = 1$, are the instantaneous volume fractions of the solid and fluid phases, respectively; p is the fluid pressure; the superscripts s and f imply the solid and fluid phase, respectively. The elastic stress, $\tilde{\sigma}^s{}_0$, is determined using Eq.(4).

The equation of motion of the tissue is governed by:

$$\begin{aligned} \nabla \cdot \tilde{\sigma}^s + \tilde{\pi}^s &= 0 \\ \nabla \cdot \tilde{\sigma}^f + \tilde{\pi}^f &= 0 \end{aligned} \tag{6}$$

where $\tilde{\pi}^f$ and $\tilde{\pi}^s$ are the momentum exchanges, given by:

$$\tilde{\pi}^f = -\tilde{\pi}^s = \Phi^s \nabla p + K\left(\tilde{v}^s - \tilde{v}^f\right) \tag{7}$$

where $\tilde{v}^f$ and $\tilde{v}^s$ are the speed of the fluid and solid phases, respectively; K is the diffusive drag constant, which measures the frictional resistance of the fluid flowing through the solid matrix and is related to the hydraulic permeability, k, by $K=(\Phi^f)^2/k$.

The hydraulic permeability is considered to be deformation-dependent (Holmes and Mow, 1990; Wu and Herzog, 2000):

$$k = k_0\left(\frac{e}{e_0}\right)^{\kappa} \exp\left\{\frac{M}{2}\left[\left(\frac{1+e}{1+e_0}\right)^2 - 1\right]\right\} \tag{8}$$

where e and e_0 are the void ratios in the deformed and undeformed state, respectively; M and κ are the material parameters.

The Young's moduli of the bone and nail were assumed according to the published experimental data (Yamada, 1970) to be 17.0 GPa and 170.0 MPa, respectively, while Poisson's ratio was assumed to be 0.30 for both. The material parameters of the skin and subcutaneous tissues used in the present simulations were determined based on the published experimental data (Pan et al., 1998; Wan, 1994; Zhen and Mak, 1996).

Material parameters characterizing hyperelasticity and viscoelasticity for the skin (ν=0.40)

i	1	2	3
α_i	4.941	6.425	4.712
μ_i (MPa)	$-7.594\text{X}10^{-2}$	$1.138\text{X}10^{-2}$	$6.572\text{X}10^{-2}$
g_i	0.148	0.252	--
τ_i (s)	2.123	9.371	--

Material parameters characterizing the hyperelasticity for the subcutaneous tissue (ν=0.40)

i	1	2	3
α_i	5.511	6.571	5.262
μ_i (MPa)	$-4.895\text{x}10^{-2}$	$9.889\text{x}10^{-3}$	$3.964\text{x}10^{-2}$

Material parameters of hydraulic permeability for the subcutaneous tissue

M	κ	k_0 (m^4/Ns)	e_0
4.638	0.0848	$1.0\text{x}10^{-15}$	1.5

Clemente, C.D. (1981) Anatomy: A regional atlas of the human body (2 ed.).Baltimore-Munich: Urban and Achwarzengerg.

Guyton, A. (1982). Human Physiology and Mechanisms of Disease (3rd ed.). W.B. Saunders Co., Philadelphia.

Harada, N. and M.J. Griffin (1991). Factors influencing vibration sense thresholds used to assess occupational exposures to hand transmitted vibration. British Journal of Industrial Medicine, 48(3), 185-92.

Holmes, M. and V.C. Mow (1990). Nonlinear characteristics of soft gels and hydrated connective tissues in ultrafiltration. J. Biomech. 23, 1145-1156.

ISO/FDIS-13091-1 (2001). International standard: Mechanical vibration - Vibrotactile perception thresholds for the assessment of nerve dysfunction -- Part 1: Methods of measurment at the fingertips. Technical report, The International Organization For Standardization.

Morrissey, S., F. Winn, and A. Bittner (1996). Screening for carpal tunnel syndrome with vibration threshold testing. Technical report, Ergonomics Society of Taiwan.

Mow, V.C., S.C. Kuei, W.M. Lai, and C.G. Armstrong (1980). Biphasic creep and stress relaxation of articular cartilage: theory and experiment. ASME J. Biomech. Eng. 102, 73-84.

Pan, L., L. Zan, and F. Foster (1998). Ultrasonic and viscoelastic properties of skin under transverse mechanical stress in vitro. Ultrasound Med Biol 24(7), 995-1007.

Perez, C., C. Holzmann, and H. Jaeschke (2000). Two-point vibrotactile discrimination related to parameters of pulse burst stimulus. Med Biol Eng Comput 38(1), 74-9.

Phillips, J. and K. Johnson (1981). Tactile spatial resolution. {III.} a continuum mechanics model of skin predicting mechanoreceptor responses to bars, edges, and gatings. J Neurophysiol 46(6), 1204-25.

Rubin, M., S. Bodner, and N. Binur (1998). An elastic-viscoplastic model for excised facial tissues. J Biomech Eng 120(5), 686-9.

Serina, E., E. Mockensturm, C.J. Mote, and D. Rempel (1998). A structural model of the forced compression of the fingertip pulp. J Biomech 31(7), 639-46.

Srinivasan, M. and K. Dandekar (1996). An investigation of the mechanics of tactile sense using two-dimensional models of the primate fingertip. J Biomech Eng 118(1), 48-55.

Srinivasan, M. and R. LaMotte (1987). Tactile discrimination of shape: responses of slowly and rapidly adapting mechanoreceptive afferents to a step indented into the monkey fingerpad. J Neurosci 7(6), 1682-97.

Storakers, B. (1986). On material representation and constitutive branching in finite conpressible elasticity. J Mech Phys Solid 34(2), 125-145.

Tschoegl, N.W. (1989). The phenomenological theory of linear viscoelastic behavior: An introduction. Springer-Verlag.

Verrillo, R.T. and G.A. Gescheider (1977). Effect of prior stimulation on vibrotactile thresholds. Sensory Processes 1 , 292-300.

Wan, A.W. (1994). Biaxial tension test of human skin in vivo. Biomed Mater Eng 4(7), 473-486.

Wu, J. and W. Herzog (2000). Finite element simulation of location- and time-dependent mechanical behavior of chondrocytes in unconfined compression tests. Ann Biomed Eng 28(3), 318-30.

Yamada, H. (1970). Strength of biological materials. Baltimore: Williams and Wilkins Co.

Zheng, Y. and A.M. Mak (1996) An ultrasound indentation system for biomechanical properties assessment of soft tissues in-vivo. IEEE Trans Biomed Eng 43(9), 912-8.